



Published in final edited form as:

Invest Ophthalmol Vis Sci. 2008 May ; 49(5): 1843–1849.

Zeb1 Mutant Mice as a Model of Posterior Corneal Dystrophy

Yongqing Liu^{1,2}, Xiaoyan Peng¹, Jinlian Tan³, Douglas S. Darling³, Henry J. Kaplan¹, and Douglas C. Dean^{1,2}

¹ Department of Ophthalmology and Visual Sciences, University of Louisville Health Sciences Center, Louisville KY 40202

² James Graham Brown Cancer Center, University of Louisville Health Sciences Center, Louisville KY 40202

³ Departments of Peiodontics, Endodontics and Dental Hygiene; Center for Oral Health and Systemic Disease, University of Louisville School of Dentistry, Louisville, KY 40292

Abstract

Purpose—The zinc finger transcription factor, *Zeb1*, binds to E-box like sequences and is important for maintaining repression of epithelial specification genes in vivo. Overexpression of *Zeb1* in cancer triggers epithelial-mesenchymal transition, which facilitates metastasis. Mutation of *ZEB1* in humans is linked to posterior polymorphous corneal dystrophy (PPCD), where an epithelial transition of the corneal endothelium is associated with abnormal endothelial proliferation. The purpose of this study is to determine whether *Zeb1* null or heterozygous mice may provide an animal model for PPCD.

Methods—Corneal morphology, protein and mRNA expression and cell proliferation were compared in wild-type and *Zeb1* gene knockout mice by immunostaining, real time PCR and BrdU incorporation. mRNA expression in isolated embryo fibroblasts derived from wild-type, *Zeb1* heterozygous and null mice was analyzed by real time PCR

Results—*Zeb1* null mice late in gestation show ectopic expression of epithelial genes in the corneal endothelium and keratocytes, including the basement membrane component, COL4A3, which is ectopically expressed by the corneal endothelium in PPCD. These embryos also show abnormal corneal endothelial and keratocyte proliferation, corneal thickening, and corneolenticular and iridocorneal adhesions. Adult *Zeb1* heterozygous mice exhibit these same corneal defects. The ectopic expression of epithelial genes extended to embryonic fibroblasts derived from *Zeb1* heterozygous and null mice, suggesting that *Zeb1* may have a more general role in suppression of an epithelial phenotype.

Conclusions—We conclude that *Zeb1* heterozygous and null mice show features of PPCD, and thus should provide an animal model for genetic dissection of pathways contributing to the disease.

INTRODUCTION

Posterior polymorphous corneal dystrophy (PPCD; also known as PPMD) is autosomal dominant and bilateral, and it is characterized by transition of the corneal endothelium to an epithelial phenotype, hyperplasia of the endothelium, disrupted Descemet's membrane, opacities, iridocorneal adhesions, corneal edema, corectopia and secondary glaucoma^{1–6}. There appears to be incomplete penetrance in PPCD, leading to a wide spectrum of clinical outcomes in affected families (e.g., all or only a portion of defects listed above).

Address correspondence to: Douglas C. Dean, Lions Eye Center, University of Louisville Health Sciences Center, 301 E. Muhammad Ali Blvd., Louisville KY, 40202, dcdcan01@louisville.edu.

Several different genes have been linked to PPCD, leading to subclassification of the disease based on gene mutation. PPCD1 has been reported to occur with mutation of the visual systems homeobox 1 gene (*VSX1*); however, more recent studies appear to exclude the *VSX1* locus⁷⁻⁹. PPCD2 appears to occur from mutation of the *COL8A2* gene, which encodes the $\alpha 2$ chain of type VIII collagen, a major component of Descemet's membrane. But thus far, only a single mutation has been identified in two related patients¹⁰. Gene mutations in the zinc finger homeodomain transcription factor *ZEB1* (also known as *TCF8*) are linked to PPCD3 (ref. 6-11). Indeed, in these studies it was estimated that *ZEB1* mutations may be responsible for half of all PPCD cases⁶. Accordingly, a recent study of 10 unrelated Czech and British families found that four of the families carried *ZEB1* mutations¹¹. No linkage to either *COL8A2* or *VSX1* was found, suggesting that an unknown mutation is responsible for PPCD in the other six families. Mutations in type IV collagen genes such as *COL4A3*, *COL4A4*, and *COL4A5* lead to basement membrane defects and cause the fibrotic hereditary renal disease known as Alport's syndrome, which can also be associated with PPCD¹². *COL4A3* expression was found to be deregulated in the cornea in PPCD, and *COL4A3* contains consensus binding sites for *ZEB1* in its promoter, leading to a potential scenario whereby mutation of *ZEB1* causes depression of *COL4A3*, and in turn an altered Descemet's membrane (which is normally comprised primarily of type VIII collagen)⁶.

Zeb1 is an E-box binding transcription factor whose function is closely linked to TGF- β signaling. It binds to activated Smads (the downstream TGF- β family signaling molecules) facilitating their assembly into a transcriptionally active complex with the transcriptional co-activator, p300, thereby augmenting TGF- β -mediated signaling¹³. But in the absence of TGF- β signaling, *Zeb1* can interact with the transcriptional repressor, CtBP, to repress transcription¹⁴. Overexpression of *Zeb1* in cancer triggers epithelial-to-mesenchymal transition (EMT) (reviewed in ref. 15), a TGF- β -dependent process which facilitates metastasis^{16,17}. This cancer EMT is the result of *Zeb1*-mediated repression of epithelial specification genes such as E-cadherin and genes involved in polarity and tight junction formation. Conversely, *Zeb1* null mice show an opposite phenotype: expansion of the pattern of epithelial gene expression, and loss of mesenchymal gene expression¹⁸, and *Zeb1* heterozygous mice have diminished TGF- β -dependent signaling leading to defects in smooth muscle differentiation following vascular injury¹⁹. These properties suggest a model whereby mutation of *ZEB1* may be responsible for ectopic expression of epithelial genes in corneal endothelium, leading to the epithelialization of the cells in PPCD.

Here, we examined *Zeb1* heterozygous and null mice to determine whether these mutant mice might provide an animal model of PPCD. We found that the cornea became thickened in late-stage null mouse embryos with epithelialization of the endothelium and keratocytes, as evidenced by ectopic expression of epithelial markers such as cytokeratin, E-cadherin and *COL4A3*. There were iridocorneal and corneolenticular adhesions, consistent with dysfunctional corneal endothelium. Additionally, this epithelialization of the corneal endothelium was associated with abnormal proliferation of the cells as occurs in PPCD^{6,20}. We found a similar posterior corneal phenotype in adult heterozygous mice. These results suggest that *Zeb1* mutant mice may provide an important tool for analysis of pathways involved in PPCD.

MATERIALS AND METHODS

Mouse cornea and MEF isolation and culture

Zeb1 heterozygous mice²¹ in a C57BL/6 background were maintained as a colony by breeding with wild-type C57BL/6 mice. Heterozygotes were mated to obtain *Zeb1* null embryos. Mouse genotyping was conducted as described²¹. All animals were handled according to the regulations of the Institutional Animal Care and Use Committee, and all procedures adhered

to the tenets of the ARVO Statement for the Use of Animals in Ophthalmic and Vision Research.

Embryonic corneas and fibroblasts (MEFs) were isolated from E18.5 and E13.5 mouse embryos, respectively. For MEF isolation, corneal dissection and for Immunostaining below, pregnant mice were exposed to CO₂ and embryos were surgically harvested. A routine MEF isolation procedure was used: the head and visceral organs were removed, and the remaining body cavity was minced and trypsinized. MEFs were cultured in 10% CO₂ at 37°C in DMEM supplemented with 10% heat-inactivated fetal bovine serum, and cells were split 1:3 as they became confluent. For corneal isolation, eyes were removed after embryo harvest, and corneas were dissected from the eyes under a dissecting scope. Isolated corneas were immediately frozen in liquid nitrogen. Corneas of the same genotype were pooled.

RNA extraction and real-time PCR

Total RNA from corneas or cultured MEFs was isolated using Trizol solution (Invitrogen, Carlsbad, CA). cDNA was synthesized using the Invitrogen RT kit according to the manufacturer's protocol (Invitrogen, Carlsbad, CA).

Using Primer3 (<http://frodo.wi.mit.edu/cgi-bin/primer3/primer3.cgi>), primer sets were designed to generate 100–200 base pair PCR products that bridged two separate exons. Primer sequence, melting temperature (T_m), and PCR product sizes are listed in the Supplementary Table. Real-time PCR was performed in 25- μ l reactions containing 0.25- μ l aliquots of cDNA, gene-specific primers, and SYBR Green I fluorescent dye (Molecular Probes, Eugene, Oregon), in an Mx3000P Real-Time PCR System (Stratagene, Cedar Creek, Texas). Parameters were set at 95°C for 20 sec, 60°C for 30 sec, and 72°C for 30 sec, for a total of not more than 45 cycles. The fluorescent intensity of SYBR Green was monitored at the end of each extension step; relative amounts of the target cDNA was estimated by the threshold cycle (C_t) number, and compared to two control genes, β -actin and glyceraldehyde-3-phosphate dehydrogenase (GAPDH). Three independent samples were analyzed for each condition and/or cell type, and each sample was compared in at least 3 independent amplifications.

Immunohistochemistry

Mouse embryos or enucleated adult eyes were fixed in 10% buffered formalin, embedded in paraffin, and sectioned at 5 μ m. These sections were used for H&E staining or for immunofluorescence. For immunofluorescent staining, the primary antibody dilution for Zeb1 (raised against the central homeodomain region of the protein expressed in bacteria, and then used to immunize rabbits)²², COL4A3 (mAb 8D1, from D.B. Borza, Vanderbilt University)²³; cytokeratin (Biolegend, San Diego, CA), E-cadherin (BD-Pharmingen, San Jose, CA) was 1:100, 1:10, 1:10, and 1:50, respectively, whereas the secondary antibody dilution was 1:300 for both anti-rabbit IgG conjugated with Alex Fluor®-488 (Molecular Probes, Eugene, Oregon) and anti-mouse IgG conjugated with Cy3 (Sigma, St. Louis, MO). The slides were mounted with coverslips using anti-fade medium Permount and viewed under a Zeiss confocal microscope. The same exposure time was used to capture images of wild-type and null embryo sections. Images were captured and assembled using Zeiss LSM5 Image Examiner software. Then, images were transferred to a Powerpoint file to create the figures. The Powerpoint file was then converted to a PDF document.

BrdU incorporation assays

Two hours before collection of embryos at E13.5 or E15.5, mothers received an intraperitoneal injection of 40 mg/kg of 5'-bromodeoxyuridine (BrdU) in PBS. Embryos were fixed, embedded in paraffin, and sectioned at 5 μ m. Sections were incubated with 0.1% Tween 20, 4% sheep serum, and 2% bovine serum albumin (BSA) (Sigma, St. Louis, MO) for 1 hr. Primary antibody

against BrdU²² was applied to the sections at 1:50, and incubated at 4°C overnight. Slides were then incubated at 1:300 dilution either with anti-mouse IgG conjugated to Cy3 (Sigma, St. Louis, MO) or with horseradish peroxidase-conjugated anti-mouse IgG antibody (1:5000) in 1% (vol/vol) normal goat serum in PBS for 1 hr, washed three times for 5 min each in PBS, and then developed using DAB peroxidase reagents. The slides were viewed with a Zeiss confocal microscope, and images were captured and processed as described above under Immunohistochemistry.

To quantify BrdU incorporation, at least 50 cells were counted for corneal endothelium, corneal epithelium, keratocytes and lens epithelium, and the percentage of BrdU-positive cells determined. Litter mates were used for these studies. At least two different mice were used for each genotype and age, and 5 adjacent 5 micron sections were counted for each mouse. The region of the corneas assessed is shown in Fig. 5A and C.

Corneal thickness measurements

Corneal thickness was measured in H&E stained sections of the different *Zeb1* genotypes and at different ages. Litter mates were used for these studies. At least two different mice were used for each genotype and age, and 5 adjacent 5 micron sections were counted for each mouse. The region of the cornea measured is shown in Fig. 5A and C.

Corneal keratocyte nuclei were counted in adult (4 months) wild-type and heterozygous litter mates. Three mice were used for each genotype. The same regions used to determine corneal thickness were used to count keratocyte nuclei. Keratocyte nuclei were counted in a 200 μM linear region of the corneas. To do this, a 200 μM square box was placed on the corneal image, and keratocyte nuclei within the box were counted. The edge of the box was placed on the corneal epithelium. As a control, corneal epithelial nuclei were counted in the same box.

RESULTS

Expression of epithelial markers in corneal endothelium and keratocytes in *Zeb1* null embryos

Zeb1 null mice die at birth from a failure to initiate respiration²¹, thus they cannot be analyzed postnatally. Therefore, we began by examining corneas in wild-type and *Zeb1* null mice near the end of gestation. Immunostaining for *Zeb1* showed expression in the corneal endothelium, as well as stromal keratocytes; no expression was evident in the corneal epithelium (Fig. 1A–A'). Epithelial markers including E-cadherin, pan cytokeratin, and COL4A3 were absent from the corneal endothelium and keratocytes, but were evident on epithelium of the cornea, lens and eye lid (as well as the skin) (Fig. 1B–B', C–C', D–D'; results not shown).

Next, we asked whether there is evidence of an epithelialization of corneal endothelium and keratocytes in *Zeb1* null mice (e.g., do the epithelial markers become ectopically expressed on corneal endothelium and keratocytes in *Zeb1* null mice?). *Zeb1* null litter mates at E16.5 were then immunostained for COL4A3, cytokeratin and E-cadherin. Each of these epithelial markers became ectopically expressed on the corneal endothelium in *Zeb1* null mice, and COL4A3 and cytokeratin were also evident on keratocytes in the null mice (Fig. 1E–E', F–F', G–G'). While these epithelial markers became ectopically expressed on corneal endothelium and on keratocytes in the null mice, their expression on corneal epithelium or on the epithelium of the lens, eye lid or skin did not diminish in the null mice. These results indicate that *Zeb1* is required to prevent expression of epithelial specification genes on corneal endothelium and keratocytes, but loss of *Zeb1* does not affect expression of these markers on epithelial cells (where *Zeb1* is not expressed). As a negative control, immunostaining for each of the proteins was dependent

on the primary antibody, and importantly we also found that the *Zeb1* null mutation eliminates *Zeb1* immunostaining in the eye at E16.5 (results not shown).

COL4A3 and E-cadherin mRNAs are induced late in gestation in the cornea of *Zeb1* null mice, but not *Zeb1* heterozygotes

Next, we dissected corneas from wild-type, heterozygous and null litter mates at E18.5, and compared the level of mRNA expression for COL4A1, COL4A3, and E-cadherin, (using both β -actin and GAPDH mRNAs as controls). As with protein expression, we found significant induction of COL4A3 and E-cadherin mRNAs using real time PCR in the corneas of *Zeb1* null mice (Fig. 2). There was only a modest increase in COL4A1 mRNA in the null corneas. Little difference in mRNA levels was evident between wild-type and heterozygous corneas at this developmental stage.

Increased proliferation of the corneal endothelium and keratocytes late in gestation in *Zeb1* null mice

Epithelialization of the corneal endothelium in PPCD is associated with abnormal cell proliferation. We noticed that corneas from *Zeb1* null mice at E15.5 and E17.5 appeared thicker than their wild-type litter mates (Fig. 3A; also shown in Fig. 5 below), suggesting that the *Zeb1* null corneas may be undergoing abnormal proliferation to add cells to the cornea. To assess proliferation in the cornea, pregnant mice at E13.5 and E15.5 were injected with BrdU two hrs prior to harvesting embryos. BrdU incorporation, as a measure of cell proliferation, was then analyzed by immunostaining in sections of wild-type and null litter mates. Proliferation was evident throughout the cornea in both wild-type and *Zeb1* null mice at E13.5 (Fig. 3B). However, proliferation became largely restricted to the epithelium in wild-type corneas by E15.5 (Fig. 3A). While the corneal epithelium and lens epithelium remained proliferative in the null mice at E15.5, endothelial cells and keratocytes were also proliferative in the null corneas (Fig. 3A). Thus, ectopic expression of epithelial markers on the corneal endothelium and keratocytes in *Zeb1* null mice is associated with abnormal proliferation of these cells at E15.5.

***Zeb1* null mice show increased corneal thickness, and corneolenticular, iridocorneal, and iridolenticular adhesions late in gestation**

Consistent with increased proliferation in the corneas of *Zeb1* null late stage embryos, corneas from *Zeb1* null mice at E17.5 were thicker than corneas from their wild-type litter mates, and this was due at least in part to an increase in the number of keratocytes (Fig. 4A and B). Corneal thickness in heterozygous mice was not statistically different from wild-type. By contrast, corneas from wild-type and *Zeb1* null mice at E13.5 (where corneal proliferation was similar; Fig. 3B) showed similar thicknesses (Fig. 4A).

In addition to increased corneal thickness, iridocorneal, corneolenticular, and iridolenticular adhesions were evident in *Zeb1* null mice at E17.5 (Fig. 5A–F). These corneolenticular adhesions frequently led to corneal disruption, with the endothelium torn away from the cornea and adherent to the lens epithelium (Fig. 5E). Iridocorneal adhesion led to loss of the iridocorneal angle in the null embryos (Fig. 5C–D). Such pathologic defects are indicative of defective corneal endothelium, and are associated with posterior corneal dystrophies such as PPCD.

Corneal thickening and iridocorneal and corneolenticular adhesions in adult *Zeb1* heterozygous mice

We did not detect obvious corneal defects in late-stage *Zeb1* heterozygous embryos, despite the fact that heterozygous *ZEB1* mutation is linked to human PPCD. However, corneal defects

in the null mice only became evident late in embryogenesis (implying an age-dependent effect), and in patients PPCD is frequently not diagnosed until 20–30 years of age²⁰. Therefore, we examine adult (4 months) *Zeb1* heterozygous mice for corneal defects. Corneal thickening and increased keratocyte number were evident in the heterozygous mice compared to wild-type litter mates (Fig. 4A and B). The relative increase in corneal thickness in the adult heterozygotes was similar to that observed in late-stage null embryos.

As with late-stage *Zeb1* null embryos, adult *Zeb1* heterozygotes showed both iridocorneal and corneolenticular adhesions (Fig. 6A–A', B–B'). And also as with *Zeb1* null embryos, these iridocorneal adhesions led to loss of the iridocorneal angle (Fig. 7).

COL4A3 mRNA is induced in a *Zeb1* gene dosage dependent fashion in embryo fibroblasts

Zeb1 is crucial for suppressing an epithelial phenotype in mesenchymal and neuroectodermal cells in vivo¹⁸. Indeed, we have found that E-cadherin becomes expressed in a *Zeb1* dosage-dependent fashion in embryonic fibroblasts¹⁸ (Fig. 8), and this induction of E-cadherin is associated with transition of the *Zeb1* null embryonic fibroblasts to epithelial morphology¹⁸. Therefore, we wondered whether *Zeb1* gene mutation might also lead to induction of COL4A3 mRNA (*COL4A3* is proposed to be a target of *Zeb1* repression whose ectopic expression in corneal endothelium and keratocytes is important in PPCD⁶). Fibroblasts were isolated from wild-type, heterozygous, and null litter mate embryos. And, we found using real time PCR that COL4A3 mRNA was indeed induced in heterozygous cells, and there was further induction in the null cells (Fig. 8). As controls, there was no change in expression of β -actin or GAPDH mRNAs, and relatively little change in COL4A1 mRNA was evident. As opposed to COL4A3, COL4A1 expression is not induced in the corneal endothelium or keratocytes in PPCD⁶.

DISCUSSION

Overexpression of ZEB1 in cancer triggers EMT, which facilitates metastasis in late stage carcinomas. By contrast, the opposite phenotype (de-repression of epithelial specification genes in mesenchymal, neuroectodermal, and endothelial cells) is seen in *Zeb1* null mice (ref. 18 and this study).

Zeb1 shares E-box binding sites on target gene promoters with the Snail family of transcription factors²⁴. As with *Zeb1*, Snail can be overexpressed in cancer leading to EMT^{15,25}. And *Snail1* null mice also show ectopic expression of epithelial specification genes, but as opposed to *Zeb1* null mice, this ectopic expression is seen early in embryogenesis (e.g., these defects prevent formation of the ectodermal-mesodermal boundary required for gastrulation²⁶). In *Drosophila*, Snail is responsible for repressing the *Zeb1* homologue (*zfh1*) and preventing its expression until later stages of gestation²⁷. *Zeb1* expression also follows that of Snail in mouse embryogenesis, and defects in *Zeb1* null mice are not evident until later in gestation²¹. Therefore, Snails may be functioning to suppress epithelial gene transcription early in gestation, whereas *Zeb1* assumes this role later in gestation.

It is of note that corneal endothelium and stromal keratocytes are derived from cranial neural crest, as are many of the mesenchymal cells responsible for craniofacial development (craniofacial defects are prominent in *Zeb1* null mice²¹). *Zeb1* is expressed on migrating cranial neural crest²², and our results imply that it may be important in regulating the gene expression pattern of these cells as they undergo differentiation. Further, gene expression is also altered in fibroblasts cultured from mutant embryos (an epithelialization of the cells appears to occur) and in neuroepithelial cells in vivo¹⁸, suggesting that this *Zeb1* regulation extends beyond cranial neural crest-derived cells.

Interestingly, the proliferative phenotype seen here in corneal endothelial cells and keratocytes is distinct from the proliferative defects we observed at sites of developing cartilage and in the CNS in *Zeb1* mutant embryos (also sites of developmental defects in the null mice)^{18,21}. The reason for these opposing effects on proliferation is unclear. However, it is of note that cell differentiation, survival and proliferation are closely linked to signals transmitted to the cell through adhesion receptors, such as the integrin family, whose members bind differentially to various extracellular matrix components (reviewed in ref. ²⁸). Descemet's membrane in the posterior cornea is a specialized basement membrane composed of a high percentage of type VIII collagen. However, COL4A3 becomes ectopically expressed in corneal endothelial cells and keratocytes in *Zeb1* null mice, thus potentially altering the composition of this crucial basement membrane. Alterations in extracellular matrix composition classically lead to apoptosis or phenotypic changes in cells bound to the matrices. For example, a de-differentiating EMT occurs in the renal tubular epithelium, resulting in fibrosis in Alport's Syndrome (where COL4A3 expression is altered, causing a defective tubular basement membrane; reviewed in ref. ²⁹). Normal development of the renal tubular epithelium requires a mesenchymal-epithelial transition during development³⁰. Taken together, these results suggest that epithelial-mesenchymal balance is crucial for formation and maintenance of the tubular epithelium, and this balance appears to be dependent upon extracellular matrix composition. It is then of note that PPCD has been reported in Alport's patients¹², and it appears that *Zeb1* function in epithelial-mesenchymal/endothelial balance is not confined to the corneal endothelium. Thus, it will be interesting to determine whether there are renal defects in *Zeb1* null mice, and whether patients showing linkage between Alport's Syndrome and PPCD have mutations in *ZEB1*.

Finally, it is of note that *Zeb1* function in vivo is linked to TGF- β signaling; it binds to activated Smads facilitating their assembly into a transcriptionally active complex with p300 (ref. 13). Heterozygous mutation of *Zeb1* leads to defective TGF- β -dependent smooth muscle gene expression and smooth cell differentiation in vivo¹⁹. Classically, epithelial vs. mesenchymal balance in cancer and in normal development is dependent upon signaling through the TGF- β family of proteins (e.g., TGF- β drives EMT)^{16,17}. It is also of note that TGF- β signaling establishes and maintains cell cycle arrest in differentiating cells via induction of cyclin dependent kinases³¹. Thus, both the epithelial phenotype and the abnormal proliferation seen in the corneal endothelium and keratocytes of the *Zeb1* null mice may prove to be associated with defective TGF- β signaling in the absence of *Zeb1*. Numerous mouse mutations in genes in the TGF- β family signaling pathway, as well as other pathways, are available for crossing with the *Zeb1* heterozygous and null mice. Thus, *Zeb1* mutant mice may provide a model to genetically dissect the pathway(s) affected in posterior corneal dystrophy.

Acknowledgements

We thank G. Foulks for helpful discussions, Y. Higashi for *Zeb1* heterozygous mice, and D.-B. Borzafar for the COL4A3 antibody. The studies were supported in part by NIH Grants (RR018733, EY015636, and EY017869), Research to Prevent Blindness, and The Commonwealth of Kentucky Research Challenge.

References

1. Pearce WG, Tripathi RC, Morgan G. Congenital endothelial corneal dystrophy: clinical, pathological and genetic study. *Br J Ophthalmol* 1969;53:577-91. [PubMed: 4900143]
2. Cibis GW, Krachmer JA, Phelps CD, Weingeist TA. The clinical spectrum of posterior polymorphous dystrophy. *Arch Ophthalmol* 1977;95:1529-37. [PubMed: 302697]
3. Krachmer JH. Posterior polymorphous corneal dystrophy: a disease characterized by epithelial-like endothelial cells which influence the management and prognosis. *Trans Am Ophthalmol Soc* 1985;83:413-75. [PubMed: 3914130]

4. Heron E, Mathers WD, Alward WL, et al. Linkage of posterior polymorphous corneal dystrophy to 20q11. *Hum Mol Genet* 1995;4:485–88. [PubMed: 7795607]
5. Moroi SE, Gokhale PA, Schteingart MT, et al. Clinicopathologic correlation and genetic analysis in a case of posterior polymorphous corneal dystrophy. *Am J Ophthalmol* 2003;135:461–70. [PubMed: 12654361]
6. Krafchak CM, Pawar H, Moroi SE, et al. Mutations in TCF8 cause posterior polymorphous corneal dystrophy and ectopic expression of COL4A3 by corneal endothelial cells. *Am J Hum Genet* 2005;77:694–708. [PubMed: 16252232]
7. Heon E, Greenberg A, Kopp KK, et al. VSX1: a gene for posterior polymorphous dystrophy and keratoconus. *Hum Mol Genet* 2002;11:1029–36. [PubMed: 11978762]
8. Aldave AJ, Yellore VS, Principe AH, et al. Candidate gene screening for posterior polymorphous dystrophy. *Cornea* 2004;24:151–5. [PubMed: 15725882]
9. Gwillam R, Liskova P, Filipec M, et al. Posterior polymorphous corneal dystrophy in Czech families maps to chromosome 20 and excludes the VXS1 gene. *Invest Ophthalmol Vis Sci* 2005;46:4480–4.
10. Biswas S, Munier FL, Yardley J, et al. Missense mutations in COL8A2, the gene encoding the alpha2 chain of type VIII collagen, causes two forms of corneal endothelial dystrophy. *Hum Mol Genet* 2001;10:2415–23. [PubMed: 11689488]
11. Liskova P, Tuft SJ, Gwilliam R, et al. Novel mutations in the ZEB1 gene identified in Czech and British patients with posterior polymorphous corneal dystrophy. *Hum Mut.* 2007(in press)
12. Colville DJ, Savige J. Alport syndrome: a review of the ocular manifestations. *Ophthalmic Genet* 1997;18:161–73. [PubMed: 9457747]
13. Postigo AA. Opposing functions of ZEB proteins in the regulation of the TGFbeta/BMP signaling pathway. *EMBO J* 2003;22:2443–2452. [PubMed: 12743038]
14. Postigo AA, Dean DC. ZEB represses transcription through interaction with the corepressor CtBP. *Proc Natl Acad Sci USA* 1999;96:6683–6688. [PubMed: 10359772]
15. Peinado H, Olmeda D, Cano A. Snail, zeb, and bHLH factors in tumour progression: an alliance against the epithelial phenotype? *Nat Rev Cancer* 2007;7:415–28. [PubMed: 17508028]
16. Thiery JP. Epithelial-mesenchymal transitions in development and pathologies. *Curr Opin Cell Biol* 2003;15:740–6.
17. Zavadil J, Bottlinger EP. TGF-beta and epithelial-to-mesenchymal transitions. *Oncogene* 2005;24:5764–74. [PubMed: 16123809]
18. Liu Y, El-Naggar S, Darling DS, et al. Zeb1 links epithelial-mesenchymal transition and cellular senescence. *Development.* 2007(in press)
19. Nishimura G, Manabe I, Tsushima K, et al. Delta EF1 regulates TGF-beta signaling in vascular smooth muscle cell differentiation. *Dev Cell* 2006;11:93–104. [PubMed: 16824956]
20. Weisenthal, RW.; Streeten, B. Posterior membrane dystrophy. In: Krachmer, J.; Mannis, M.; Holland, E., editors. *Cornea-corneal and external disease: clinical diagnosis and management.* 2. 1997. p. 1063-90.
21. Takagi T, Moribe H, Kondoh H, Higashi Y. DeltaEF1, a zinc finger and homeodomain transcription factor, is required for skeleton patterning in multiple lineages. *Development* 1998;125:21–31. [PubMed: 9389660]
22. Darling DS, Stearman RP, Qi Y, Qiu MS, Feller JP. Expression of Zfh1/deltaEf1 protein in palate, neural progenitors and differentiated neurons. *Gene Expr Patterns* 2003;3:709–17. [PubMed: 14643678]
23. Kang JS, Wang XP, Miner JH, et al. Loss of alpha3/alpha4(IV) collagen from the glomerular basement membrane induces a strain-dependent isoform switch to alpha5alpha6(IV) collagen associated with longer renal survival in Col4a3^{-/-} Alport mice. *J Am Soc Nephrol* 2006;17:1962–9. [PubMed: 16769745]
24. Postigo AA, Dean DC. Differential expression and function of members of the zfh-1 family of zinc finger/homeodomain repressors. *Proc Natl Acad Sci USA* 2000;97:6391–6396. [PubMed: 10841546]
25. Hemavathy K, Ashraf SL, Ip YT. Snail/slug family of repressors, slowly going into the fast lane of development and cancer. *Gene* 2005;257:1–12. [PubMed: 11054563]

26. Carver EA, Jiang R, Lan Y, Oram KF, Gridley T. The mouse snail gene encodes a key regulator of the epithelial-mesenchymal transition. *Mol Cell Biol* 2001;21:8184–8. [PubMed: 11689706]
27. Lai ZC, Fortini ME, Rubin GM. The embryonic expression patterns of zfh-1 and zfh-2, two *Drosophila* genes encoding novel zinc-finger homeodomain proteins. *Mech Dev* 1991;34:123–134. [PubMed: 1680377]
28. Lee JW, Juliano R. Mitogenic signal transduction by integrin- and growth factor receptor-mediated pathways. *Mol Cells* 2004;17:188–202. [PubMed: 15179030]
29. Hudson BG, Tryggvason K, Sundaramoorthy M, Neilson EG. Alport's syndrome, Goodpasture's syndrome, and type IV collagen. *N Engl J Med* 2003;348:2543–56. [PubMed: 12815141]
30. Karihaloo A, Nickel C, Cantley LG. Signals which build a tubule. *Nephron Exp Nephrol* 2005;100:40–5.
31. Shi Y, Massague J. Mechanisms of TGF-beta signaling from the cell membrane to the nucleus. *Cell* 2003;113:685–700. [PubMed: 12809600]

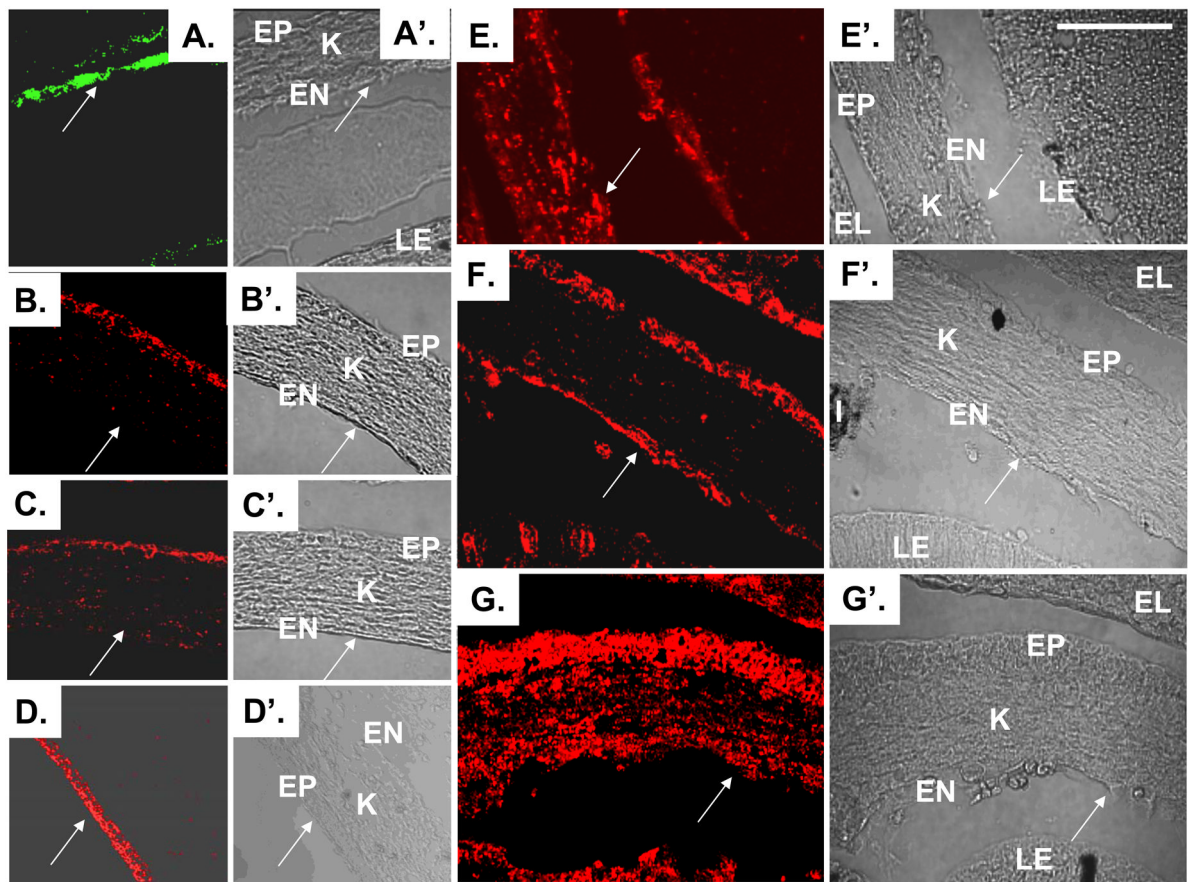


Fig. 1. E-cadherin becomes ectopically expressed in corneal endothelium, and cytokeratin and COL4A3 become ectopically expressed in corneal endothelium and keratocytes in *Zeb1* null mice. (A–A'). Immunostaining for Zeb1 is evident in corneal endothelium and keratocytes in wild-type mice. EP, corneal epithelium; EN, corneal endothelium; K, keratocytes; LE, lens epithelium. A Nomarski image is shown on the right in each panel. Arrows indicate the same location. (B–B'). Immunostaining for COL4A3 in the corneal epithelium in wild-type mice. (C–C'). Immunostaining for E-cadherin in the corneal epithelium in wild-type mice. (D–D'). Immunostaining for pan cytokeratin in the corneal epithelium in wild-type mice. (E–E'). Immunostaining for COL4A3 expands to corneal keratocytes and endothelium in *Zeb1* null mice. EL, eye lid. (F–F'). Immunostaining for E-cadherin expands to the corneal endothelium in *Zeb1* null mice. (G–G'). Cytokeratin immunostaining expands to corneal keratocytes and endothelium in *Zeb1* null mice. Sections of mice at E16.5 are shown. The bar is 100 μ m.

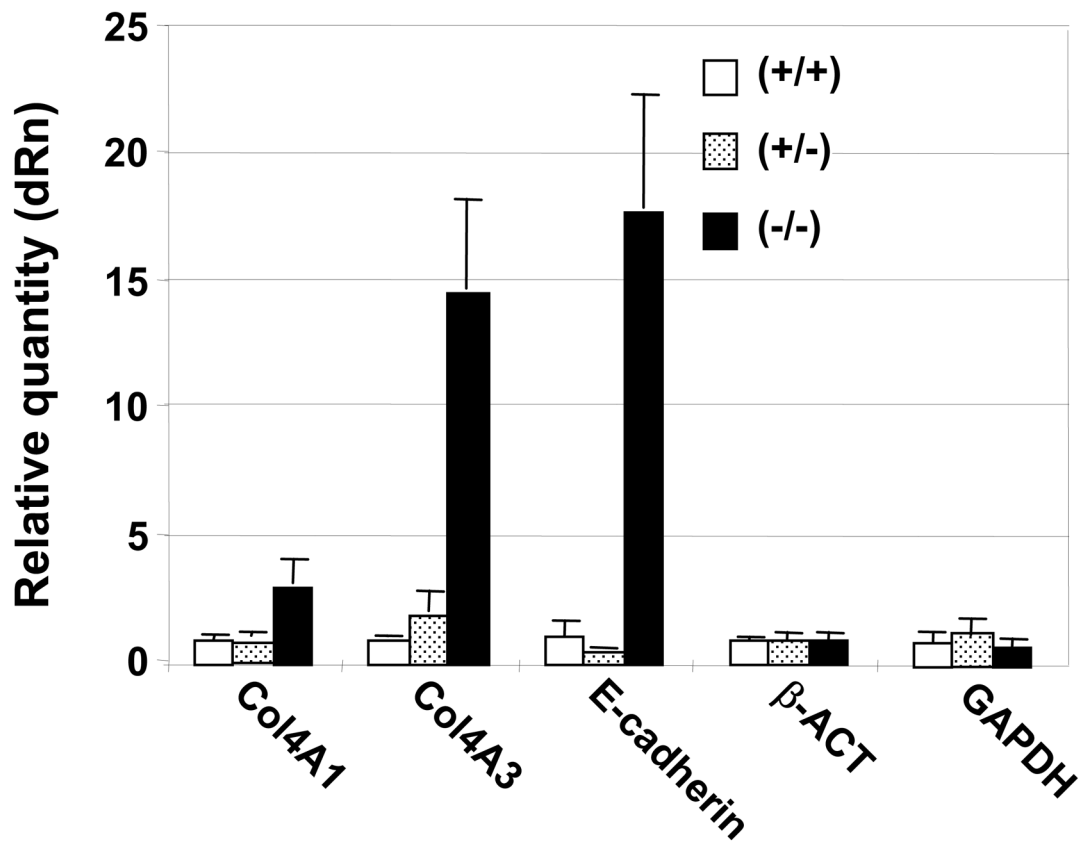
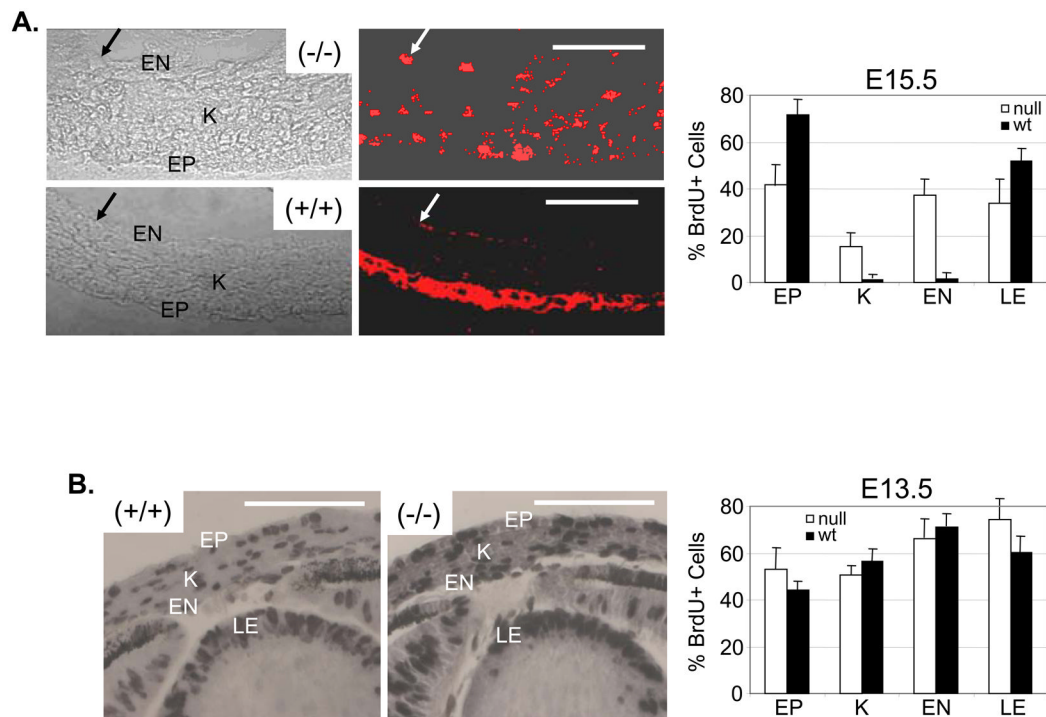


Fig. 2.

Induction of COL4A3 and E-cadherin mRNAs in the cornea in *Zeb1* null mice. mRNA levels in corneas isolated from litter mates at E18.5 were quantified by real time PCR, and compared to β -actin and GAPDH mRNAs as a control. Corneas from three embryos were pooled for each genotype.

**Fig. 3.**

Abnormal corneal proliferation occurs in *Zeb1* null mice at E15.5 but not at E13.5. Mice at E13.5 or E15.5 were injected with BrdU and embryos were harvested 2 hours later and sectioned for immunostaining with anti-BrdU antibody. **(A)**. Immunofluorescent staining for BrdU and quantification of BrdU incorporation in corneal epithelium (EP), endothelium (EN), keratocytes (K), and lens epithelium (LE) is shown at E15.5. Arrows indicate the same location in the images. Nomarski images are shown at the left in each panel. **(B)**. Immunoperoxidase staining for BrdU and quantification of BrdU incorporation into the cornea at E13.5. Bars are 100 μ m. The corneal areas counted in panels A and B are denoted below by the “*” in Fig. 5A and C. Error bars are standard deviations. Litter mates were examined, and at least two different mice were examined for each genotype, and 5 adjacent 5 micron sections were counted for each mouse.

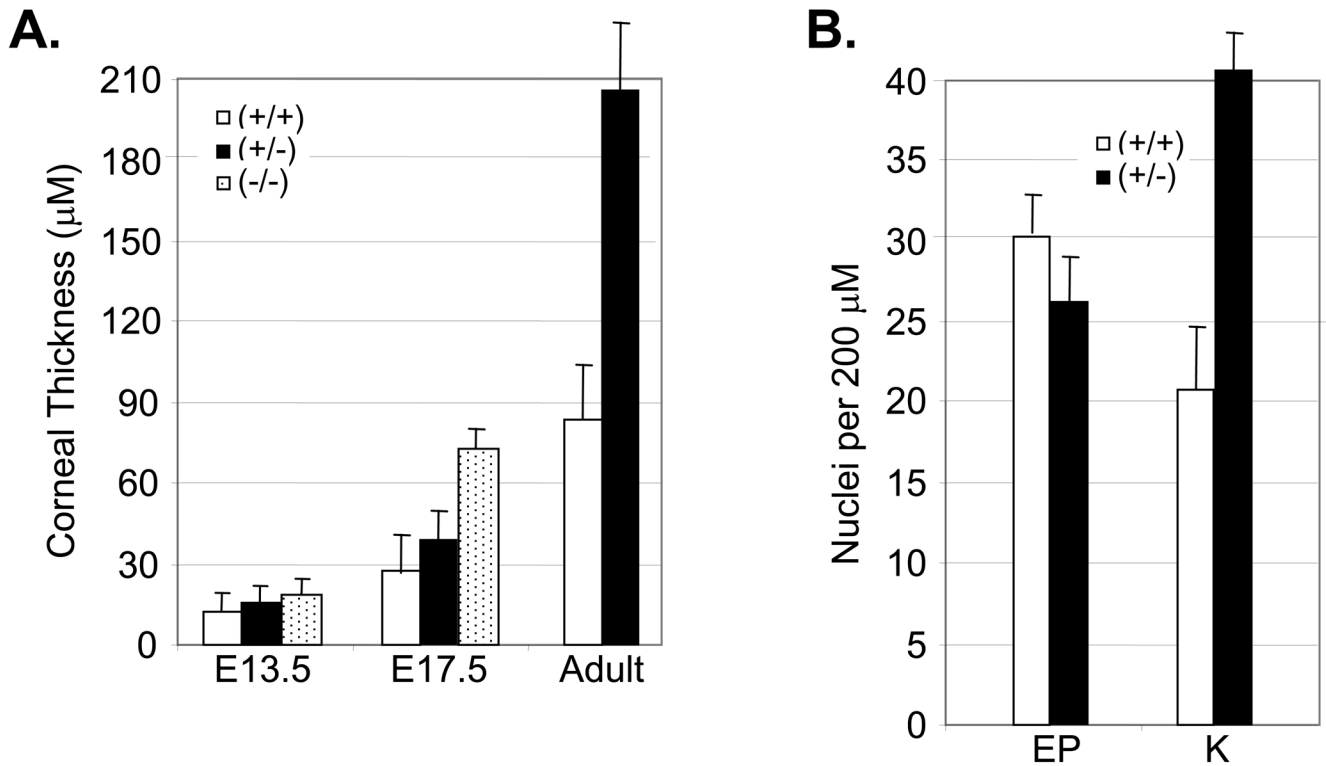


Fig. 4. Corneal thickening occurs in *Zeb1* null mice at E17.5 and in adult heterozygotes (but not in *Zeb1* null mice at E13.5), and increased keratocyte numbers is seen in heterozygous adults. (A). Corneal thickness was assessed in the regions indicated in Fig. 5A and C below. Corneal thickness was measured at E13.5, E17.5 and in 4 month old adults. (B). The number of keratocyte nuclei in a 200 μM length of cornea (in areas used to measure corneal thickness in panel A) was counted. Error bars are standard deviations. Litter mates were examined for these measurements, and at least two different mice were examined for each genotype, and 5 adjacent 5 micron sections were analyzed for each mouse.

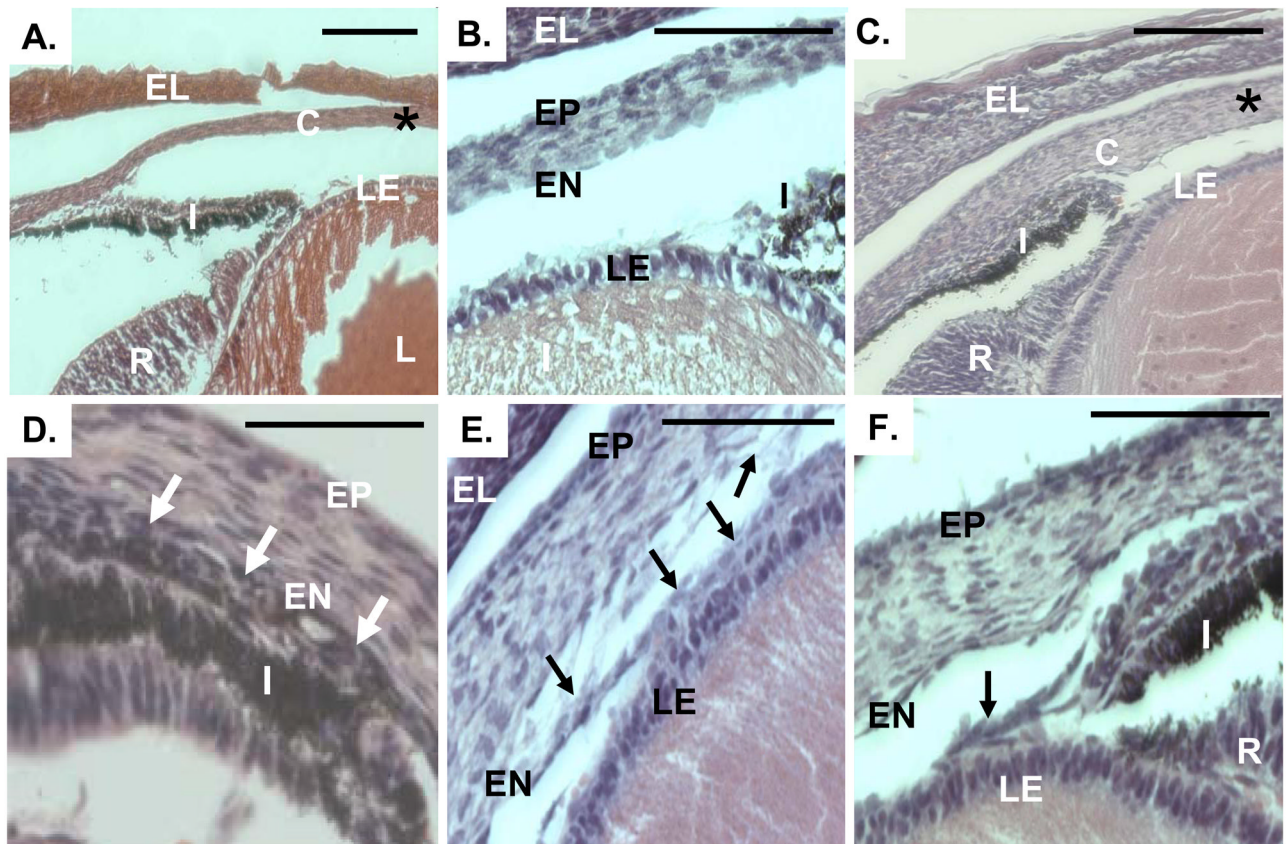


Fig. 5. Iridocorneal, corneolenticular, and iridolenticular adhesions in *Zeb1* null mice. H&E stained sections of eyes from wild type (panels A–B) and *Zeb1* null (panel C–F) mice. C, cornea; EL, eye lid; I, iris; LE, lens epithelium, R, retina; I, iris; EN, corneal endothelium; EP, corneal epithelium. The “*” in panels A and C indicates the region of the cornea analyzed for BrdU incorporation (Fig. 3) and corneal thickness (Fig. 4). Arrows in panel D indicate iridocorneal adhesion. Arrows in panels E and F show corneolenticular and iridolenticular adhesions, respectively. Bars are 100 μ m. Sections at E17.5 are shown.

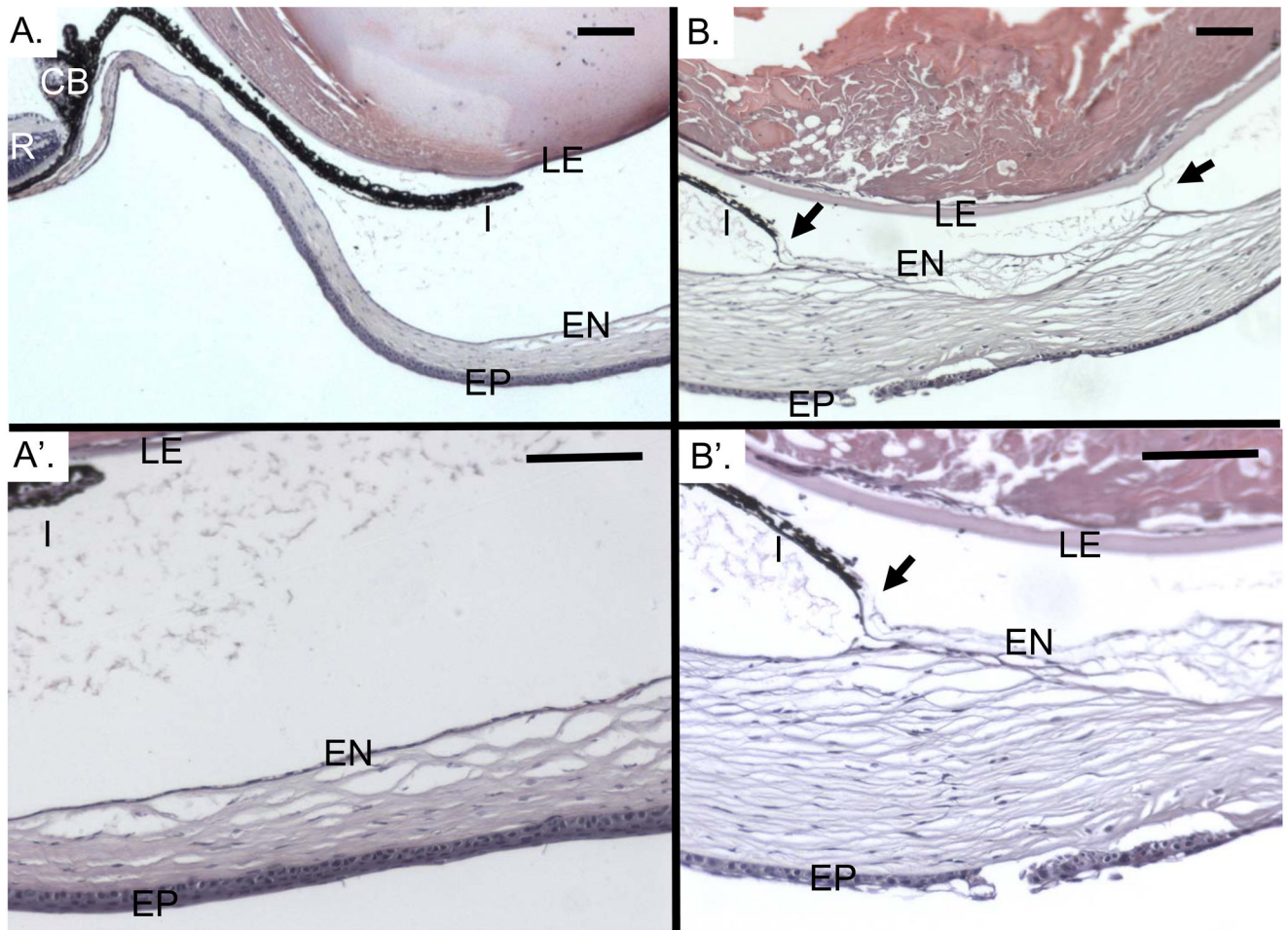


Fig. 6. Iridocorneal and corneolenticular adhesions in adult *Zeb1* heterozygous mice. H&E stained sections eyes from adult wild type (panels **A–A'**) and *Zeb1* heterozygous (panel **B–B'**) mice. Arrows in Panels **B** and **B'** show corneolenticular and iridocorneal adhesions. EP, corneal epithelium; EN, corneal endothelium, LE, lens epithelium; I, iris; R, retina; I, iris; CB, ciliary body; R, retina. Bars are 100 μ m.

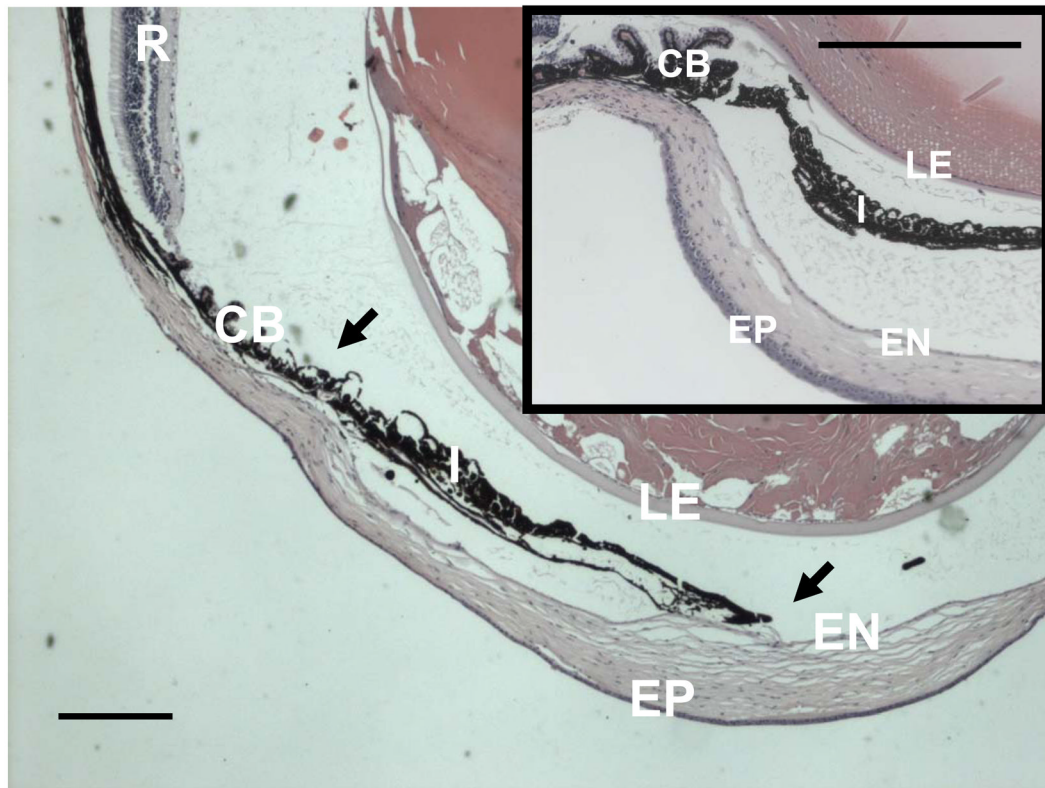


Fig. 7. Iridocorneal adhesion leads to loss of the iridocorneal angle in adult *Zeb1* heterozygous mice. H&E section through the eye of an adult *Zeb1* heterozygous mouse showing iridocorneal adhesion and loss of the iridocorneal angle. The inset shows the iridocorneal angle in a wild-type litter mate. EP, corneal epithelium; EN, corneal endothelium; LE, lens epithelium; I, iris; CB, ciliary body; R, retina. Arrows indicate iridocorneal adhesions. Bars are 200 μ m.

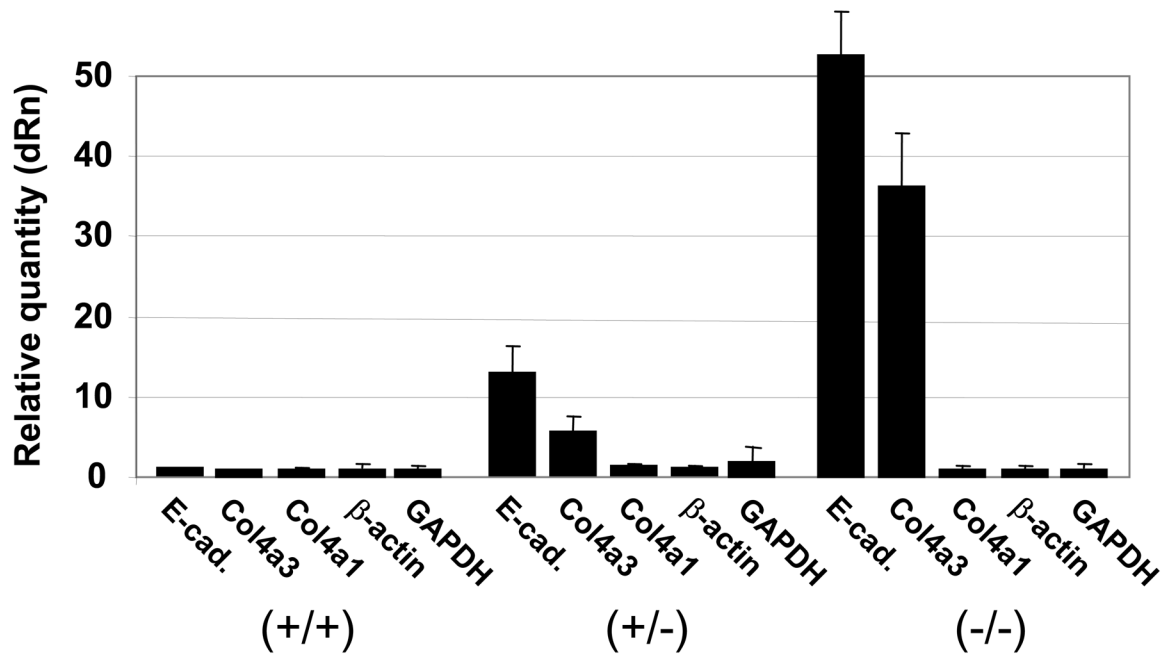


Fig. 8. Induction of epithelial genes in embryo fibroblasts derived from wild-type, *Zeb1* heterozygous and *Zeb1* null litter mates. Real time PCR analysis of mRNA levels is shown.